

# Array geometries, signal type, and sampling conditions for the application of compressed sensing in MIMO radar

Juan Lopez<sup>a</sup> and Zhijun Qiao<sup>a</sup>

<sup>a</sup>Department of Mathematics, The University of Texas - Pan American, Edinburg, Texas, 78539, USA

## ABSTRACT

MIMO radar utilizes the transmission and reflection of multiple independent waveforms to construct an image approximating a target scene. Compressed sensing (CS) techniques such as total variation (TV) minimization and greedy algorithms can permit accurate reconstructions of the target scenes from undersampled data. The success of these CS techniques is largely dependent on the structure of the measurement matrix. A discretized inverse scattering model is used to examine the imaging problem, and in this context the measurement matrix consists of array parameters regarding the geometry of the transmitting and receiving arrays, signal type, and sampling rate. We derive some conditions on these parameters that guarantee the success of these CS reconstruction algorithms. The effect of scene sparsity on reconstruction accuracy is also addressed. Numerical simulations illustrate the success of reconstruction when the array and sampling conditions are satisfied, and we also illustrate erroneous reconstructions when the conditions are not satisfied.

**Keywords:** MIMO radar, compressed sensing, basis pursuit, TV-minimization

## 1. INTRODUCTION

Multiple Input - Multiple Output (MIMO) radar imaging utilizes the transmission of spatially diverse waveforms to gather information about a desired scene. Specifically, the measurement of reflected signals is used in conjunction with the knowledge of the transmitted signals to determine an approximation of the desired scene. The collection<sup>1</sup> by Li and Stoica gives an overview of many signal processing techniques for MIMO radar imaging. The signal models presented in this collection are all linear systems based on an echolocation principle that the received data is a scaled time-delayed, and phase-shifted copy of the transmitted signal. Cheney and Borden present a model of radar imaging as an inverse problem in Maxwell's equations in<sup>2</sup> with a focus on synthetic aperture radar (SAR). This model has the advantages of a strong theoretical framework and generality. Results in compressed sensing suggest that the scene can be accurately reconstructed if the scene is sparse, that is, consists of small targets. Fannjiang in<sup>3-5</sup> gives results for the application of compressed sensing in MIMO imaging when the desired scene is sparse or consists of objects that can be approximated by piecewise constant functions; the underlying scattering model in the analysis is from.<sup>6</sup> We will apply some results by Fannjiang to give some results for basis pursuit (BP) and total variation-minimization (TV-min) in MIMO radar imaging in the case where the antennas are collocated, i.e. the transmit array is the same as the receive array.

## 2. SIGNAL MODEL

We base our analysis in the framework of Maxwell's equations. The propagation of a monochromatic plane wave  $u$  in a heterogeneous medium is governed by the scalar Helmholtz equation

$$\Delta u(\mathbf{x}) + \omega^2(1 + v(\mathbf{x}))u(\mathbf{x}) = 0, \quad \mathbf{x} \in \mathbf{R}^3, \quad (1)$$

---

J.L.: E-mail: jflopezz@utpa.edu

Z.Q.: E-mail: qiao@utpa.edu

where  $v \in \mathbf{C}$  describes the medium's inhomogeneities. Suppose that the incident wave is a plane wave  $u^i(\mathbf{x}) = \exp(i\omega\mathbf{x} \cdot d)$  with  $d \in S^2$  the incident direction. For simplicity, we assume that the speed of propagation is unity so that the frequency equals the wavenumber. The scattered field  $u^s$  then satisfies

$$\Delta u^s(\mathbf{x}) + \omega^2 u^s(\mathbf{x}) = -\omega^2 v(\mathbf{x})u(\mathbf{x}). \quad (2)$$

The scattered field has the far field asymptotic

$$u^s(\mathbf{x}) = \frac{\exp(i\omega|\mathbf{x}|)}{|\mathbf{x}|} \left( A(\hat{\mathbf{x}}, d) + O\left(\frac{1}{|\mathbf{x}|}\right) \right), \quad \hat{\mathbf{x}} = \frac{\mathbf{x}}{|\mathbf{x}|} \quad (3)$$

where  $A$  is the scattering amplitude given by

$$A(\hat{\mathbf{x}}, d) = \frac{\omega^2}{4\pi} \int_{\mathbf{R}^3} v(\mathbf{x}') [u^i(\mathbf{x}') + u^s(\mathbf{x}')] e^{-i\omega\mathbf{x}' \cdot \hat{\mathbf{x}}} d\mathbf{x}'. \quad (4)$$

$A$  is the measured data in our signal model. We linearize this model with the Born approximation by replacing  $u = u^i + u^s$  in (4) with  $u^i$  so the data model becomes

$$A(\hat{\mathbf{x}}, d) = \frac{\omega^2}{4\pi} \int_{\mathbf{R}^3} v(\mathbf{x}') u^i(\mathbf{x}') e^{-i\omega\mathbf{x}' \cdot \hat{\mathbf{x}}} d\mathbf{x}'. \quad (5)$$

### 3. POINT TARGETS AND BASIS PURSUIT

Henceforth we regard the scattering problem in  $\mathbf{R}^2$ . We first consider the case where the medium consists of  $m$  point scatterers in a square lattice of spacing  $\ell$  so that the scattering amplitude is

$$A(\hat{\mathbf{x}}, d) = \frac{\omega^2}{4\pi} \sum_{j=1}^m v_j u^i(\mathbf{x}_j) e^{-i\omega\mathbf{x}_j \cdot \hat{\mathbf{x}}} \quad (6)$$

where  $X = (v_j) \in \mathbf{C}^m$  is the target vector whose  $j$ th entry is the reflectivity of a point target at  $\mathbf{x}_j$ . We aim to establish performance guarantees on the performance of basis pursuit so that  $X$  can be recovered by solving

$$\min \|X\|_1 \quad \text{s.t.} \quad \Phi X = Y \quad (7)$$

where  $\Phi$  is the sensing matrix consisting of array parameters dependent on the geometry of data collection, sampling rate, and signal type, and  $Y$  is vector of collected data. In our analysis we consider probing signals that are plane waves  $u_k^i$  with

$$u_k^i(\mathbf{x}) = e^{i\omega(x \cos \theta_k + y \sin \theta_k)}, \quad \mathbf{x} = (x, y) \in \mathbf{R}^2, \quad (8)$$

each having incident direction determined by the angle  $\theta_k$  and each having the same frequency. We suppose that the incident angles  $\theta_k, k = 1, \dots, n$  are independent and identically distributed uniform random variables on  $[-\pi, \pi]$ . We will consider the case where the transmit and receive arrays coincide, so if  $\tilde{\theta}_k$  is a sampling angle we have  $\tilde{\theta}_k = \theta_k + \pi$ . Let  $Y_k$  be the vector of collected data due to the incident wave from the  $k$ th transmitter; the measured data is the scattering amplitude scaled by a factor of  $4\pi/\omega$ . The total data vector  $Y$  is formed by vertically stacking the  $Y_k$ 's as

$$Y = \begin{pmatrix} Y_1 \\ \vdots \\ Y_n \end{pmatrix} \in \mathbf{C}^{n^2}. \quad (9)$$

From this we can infer that the sensing matrix  $\Phi$  has  $(n(k-1) + l, j)$  entry given by

$$(\Phi)_{n(k-1)+l, j} = e^{i\omega(x_j(\cos \theta_k + \cos \theta_l) + y_j(\sin \theta_k + \sin \theta_l))} \quad (10)$$

so that  $\Phi \in \mathbf{C}^{n^2 \times m}$ . The dimension of the scene will typically be much greater than the dimension of the data, so the linear system  $Y = \Phi X$  is underdetermined. In order to successfully recover  $X$  via BP, the sensing matrix  $\Phi$  must satisfy some conditions. It is known that the coherence of  $\Phi$ , denoted by  $\mu(\Phi)$  and defined as

$$\mu(\Phi) = \max_{i \neq i'} \frac{|\sum_{j'} \Phi_{j'i} \Phi_{j'i'}^*|}{\sqrt{\sum_{j'} |\Phi_{j'i}|^2 \sum_{j'} |\Phi_{j'i'}|^2}} \quad (11)$$

affects the success of BP in recovering  $X$ . Gribonval and Nielsen<sup>7</sup> established that BP can perfectly recover  $X$  if  $X$  is  $s$ -sparse and

$$s \leq \frac{1}{2} \left( \frac{1}{\mu(\Phi)} + 1 \right). \quad (12)$$

Thus a sensing matrix with small  $\mu(\Phi)$  is desirable for recovering  $X$  by BP. Applying Fannjiang's results, we obtain the following upper bound on the sensing matrix  $\Phi$ : if

$$m \leq \frac{\delta}{8} e^{K^2/2} \quad (13)$$

for some  $\delta, K > 0$ , then

$$\mu(\Phi) < \left( \frac{n\sqrt{2}}{\sqrt{\pi\omega\ell}} + \frac{\sqrt{2}K}{\sqrt{n}} \right)^2 \quad (14)$$

with probability greater than  $(1 - \delta)^2$  and  $c = \sqrt{2/\pi}$ . Then applying the coherence result (12) we conclude that with probability greater than  $(1 - \delta)^2$  BP perfectly reconstructs  $X$  if  $X$  is  $s$ -sparse and

$$s \leq \frac{1}{2} + \frac{1}{2} \left( \frac{n\sqrt{2}}{\sqrt{\pi\omega\ell}} + \frac{\sqrt{2}K}{\sqrt{n}} \right)^{-2}. \quad (15)$$

#### 4. PIECEWISE CONSTANT TARGETS

Here we consider the case where the target scene can be approximated by piecewise constant objects. In this case

$$v(x) = \sum_{j=1}^m v_j I\left(\frac{x}{\ell} - p_j\right) \quad (16)$$

where  $I$  is the indicator function of the unit square  $[-1/2, 1/2] \times [-1/2, 1/2]$  in  $\mathbf{R}^2$  and  $p_j$  are points in the square lattice as in section 3. It is important to note that the scattering amplitude here is different than the case for a scene consisting of point targets that are clustered together. The scattering amplitude measured at sampling angle  $\phi_l$  due to the  $k$ th incident probe is given by

$$A_k(\phi_l, \omega) = \ell^2 \frac{2 \sin[(\omega\ell(\cos \theta_k - \cos \phi_l))]}{\omega\ell(\cos \theta_k - \cos \phi_l)} \frac{2 \sin[(\omega\ell(\sin \theta_k - \sin \phi_l))]}{\omega\ell(\sin \theta_k - \sin \phi_l)} \sum_p v_p e^{i\omega\ell(x_p(\cos \theta_k - \cos \phi_l) + y_p(\sin \theta_k - \sin \phi_l))} \quad (17)$$

where  $v_p = v_j \Leftrightarrow p = p_j, j = 1, \dots, m$  and  $p = (x_p, y_p)$ . We form the data vector as in the previous section; scale the  $A_k$ 's by  $4\pi/(\omega^2 g_{l,k})$  where

$$g_{l,k} = \frac{2 \sin[(\omega\ell(\cos \theta_k - \cos \phi_l))]}{\omega\ell(\cos \theta_k - \cos \phi_l)} \frac{2 \sin[(\omega\ell(\sin \theta_k - \sin \phi_l))]}{\omega\ell(\sin \theta_k - \sin \phi_l)} \quad (18)$$

and set

$$Y = \begin{pmatrix} Y_1 \\ \vdots \\ Y_n \end{pmatrix} \in \mathbf{C}^{n^2} \quad (19)$$

where each  $Y_k$  is the data collected due to the probe from  $\theta_k$ . Then we define the sensing matrix  $\Phi$  by having  $(n(k-1) + l, j)$  entry

$$e^{i\omega\ell(x_j(\cos\theta_k - \cos\phi_l) + y_j(\sin\theta_k - \sin\phi_l))} \quad (20)$$

where  $p_j = (x_j, y_j)$  and the target vector  $X$  is defined by  $(X)_j = \ell^2 v_{p_j}$ ,  $j = 1, \dots, m$ . Then the inverse problem for  $v$  can be posed as the underdetermined linear system

$$Y = \Phi X. \quad (21)$$

The main difference between this sensing matrix and the matrix used for BP is the factor of  $\ell$  in the argument of the exponential. From the results in<sup>5</sup> we conclude that TV-min can effectively recover  $X$  in the system (21) for large enough  $n$ , but still with  $n \ll m$ . The success of TV-min is illustrated in section 5.

## 5. NUMERICAL SIMULATIONS

Figure 1 shows the reconstruction of a scene with 30 point targets using basis pursuit. For comparison, the least squares estimate is also shown. The parameter values are  $\omega = 10$ ,  $n = 20$ ,  $\ell = 10$ ,  $m = 2601$ . In this case, BP has a high probability of exact reconstruction for the given level of sparsity. The BP implementation used is from Van Den Berg and Friedlander.<sup>8</sup> The results in figure 2 illustrate the failure of BP to accurately recover  $X$  when the sparsity exceed the admissible level determined by  $\mu(\Phi)$ . For this simulation, the sparsity was increased to 100 while leaving all other parameters fixed. The successful results of TV-min are given in figure 3. The same array parameter levels were used. The scene contains five extended two dimensional objects. The results in 4 illustrate the blurry reconstruction arising when the number of samples is reduced to  $n = 10$ . The implementation of TV-min used is by Li, et al.<sup>9</sup>

## 6. CONCLUSION

Here we have presented a system model for MIMO radar imaging based on the approach by Fannjiang that permits the application of the CS techniques basis pursuit and TV-min. Two of the main drawbacks of the model presented here is the formulation in two dimensions and neglecting the effects of exogenous noise. A possible extension of this approach is the application to point targets with linear velocities. We aim to apply this model to imaging moving point targets in the future.

## ACKNOWLEDGMENTS

This work was partially supported by the Texas Norman Hackerman Advanced Research Program (Grant No. 003599-0001-2009) and the U.S. Department of Education UTPA-MATH GAANN program (Grant # P200A120256).

## REFERENCES

- [1] Li, J. and Stoica, P., [*MIMO radar signal processing*], Wiley-IEEE Press (2008).
- [2] Cheney, M. and Borden, B., [*Fundamentals of radar imaging*], vol. 79, Siam (2009).
- [3] Fannjiang, A. C., "Compressive inverse scattering: I. high-frequency simo/miso and mimo measurements," *Inverse Problems* **26**(3), 035008 (2010).
- [4] Fannjiang, A. C., Strohmer, T., and Yan, P., "Compressed remote sensing of sparse objects," *SIAM Journal on Imaging Sciences* **3**(3), 595–618 (2010).
- [5] Fannjiang, A., "Compressive inverse scattering with tv-min and greedy pursuit," *arXiv preprint arXiv:1205.3834* (2012).
- [6] Colton, D. and Kress, R., [*Inverse acoustic and electromagnetic scattering theory*], vol. 93, Springer (2013).
- [7] Gribonval, R. and Nielsen, M., "Sparse representations in unions of bases," *Information Theory, IEEE Transactions on* **49**(12), 3320–3325 (2003).
- [8] Van Den Berg, E. and Friedlander, M., "Spg11: A solver for large-scale sparse reconstruction," *Online: http://www.cs.ubc.ca/labs/scl/spg11* (2007).
- [9] Li, C., Yin, W., and Zhang, Y., "Users guide for tval3: TV minimization by augmented lagrangian and alternating direction algorithms," *CAAM Report* (2009).

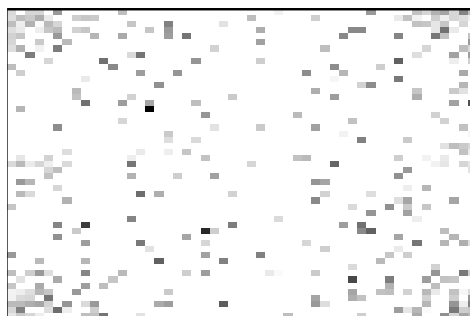
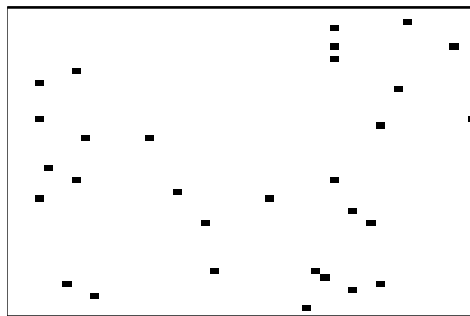
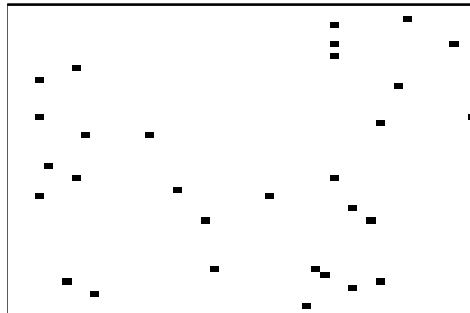


Figure 1. Scene reconstruction using basis pursuit with 30 point targets. The top is the actual scene, the middle is reconstruction using basis pursuit, and the bottom is the least squares approximation.

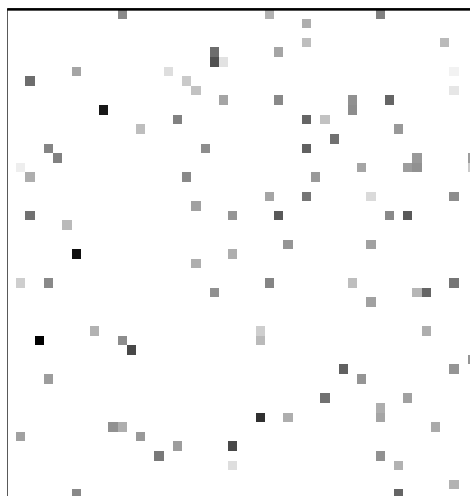
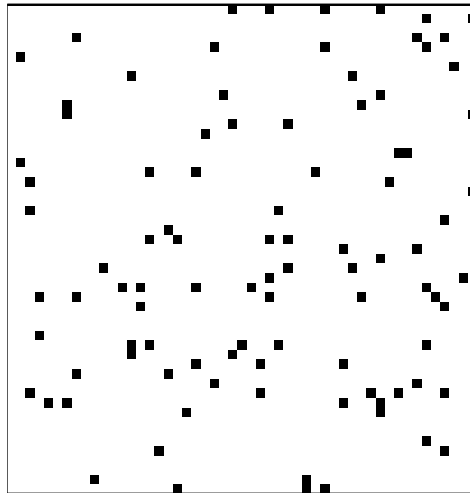


Figure 2. Scene reconstruction using basis pursuit with 100 point targets. The top is the actual scene and the bottom is the BP estimate. When the sparsity level exceeds the level permitted by  $\mu(\Phi)$  BP fails to accurately recover  $X$ .

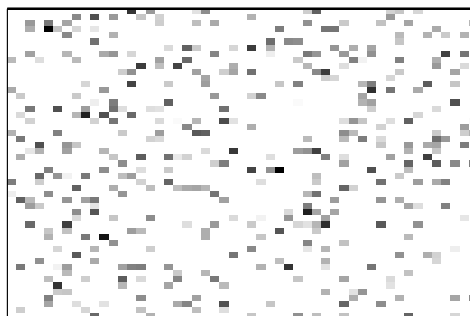
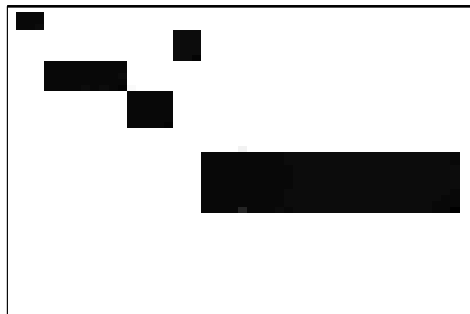
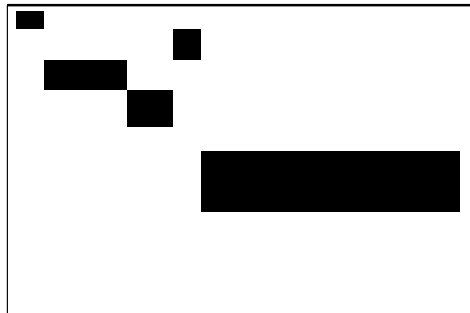


Figure 3. Scene reconstruction using TV-min with 5 piecewise constant objects. The top is the actual scene, the middle is reconstruction using TV-min, and the bottom is the least squares approximation.

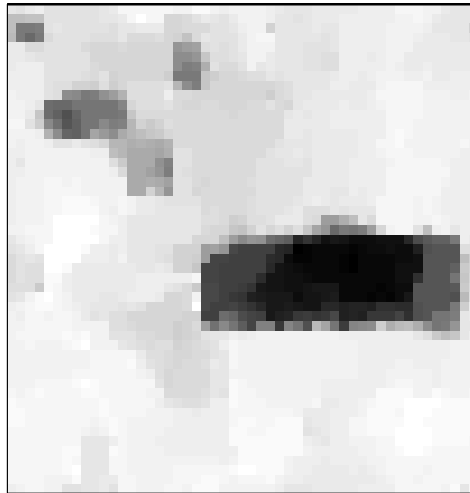
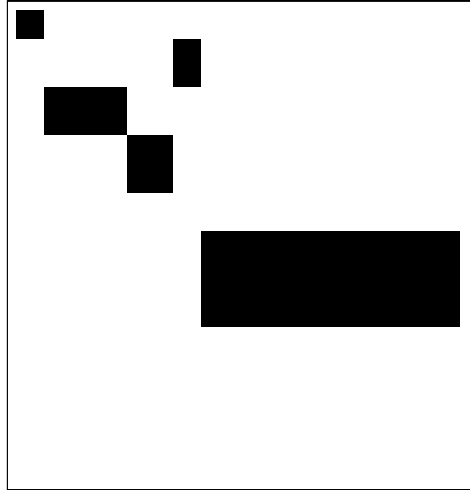


Figure 4. Blurry scene reconstruction using TV-min with 5 piecewise constant objects. The top is the actual scene and the bottom is the TV-min reconstruction.